Phase transitions and the doping effect in Ti_3O_5

1998 J. Phys.: Condens. Matter 10 7003

(http://iopscience.iop.org/0953-8984/10/31/016)

J. Phys.: Condens. Matter **10** (1998) 7003–7013. Printed in the UK PII: S0953-8984(98)92323-2

Phase transitions and the doping effect in Ti_3O_5

Masashige Onoda, Yoshihiro Ogawa and Kenji Taki
Institute of Physics, University of Tsukuba, Tennodai, Tsukuba 305-8571, Japan

Received 9 March 1998, in final form 21 April 1998

Abstract. The electronic states of the $(Ti_{1-x}V_x)_3O_5$ system, where $0 \leqslant x \leqslant 0.33$, have been explored through measurements of the x-ray diffraction, magnetization, electrical resistivity, and thermoelectric power. Three structural phases appear as the composition and temperature are varied: the high-temperature orthorhombic (HO) phase with a pseudobrookite-type structure and the slightly deformed monoclinic (HM) one, and the low-temperature monoclinic (LM) one which is completely different from the former two phases. For $0 \leqslant x \leqslant 0.08$, the HO–HM transition with a small magnetic anomaly and the HM–LM transition with significant spin-singlet Ti–Ti pairs successively take place, but for $0.1 \leqslant x \leqslant 0.33$, no transition to the LM phase exists there. While the HO-phase Ti_3O_5 is like a highly correlated metal, the HO-phase compounds with $0.1 \leqslant x \leqslant 0.33$ have a strongly localized state due to the disorder and the polaron formation, and exhibit a spin-glass-like phase at low temperatures.

1. Introduction

Transition-metal oxides and bronzes have various properties that arise from their crystal structures, which are generally formed by the linkage of polyhedral units of oxygens. In particular, 3d transition-metal oxide systems have been studied intensively to extract properties originating from a significant electron correlation, an electron–phonon coupling, or a quantum spin-fluctuation effect.

Table 1. Crystal data for Ti_3O_5 at 296, 467, and 514 K.

T (K)	Space group	Z	a (Å)	b (Å)	c (Å)	β (deg)	V (Å^3)
296	$C2/m$	4	9.748(1)	3.8013(4)	9.4405(7)	91.529(7)	349.69(6)
467	$C2/m$	4	9.835(1)	3.794(1)	9.9824(9)	90.720(9)	372.5(1)
514	$Cmcm$	4	3.798(2)	9.846(3)	9.988(4)	90	373.5(2)

Titanium binary oxides often exhibit phase transitions of crystal structures, electronic transport, or magnetic properties [1]. Among them, Ti_3O_5 which is the subject of this study undergoes first-order structural and magnetic–nonmagnetic transitions at $T_{c1} = 460$ K on heating and at $T_{c2} = 440$ K on cooling [2–14]. The crystal data for the composition Ti_3O_5 at several temperatures are listed in table 1 [14]. The low-temperature monoclinic structure below $T_{c1,2}$, hereafter called LM, has the valence order of Ti ions, in which the Ti^{3+} ($3d^1$) and Ti^{4+} ($3d^0$) sites are differentiated and the spin-singlet Ti^{3+}–Ti^{3+} pairs (dimers) are formed. Above $T_{c1,2}$, there appear two kinds of phase: one is the high-temperature monoclinic (HM) phase below $T_{mo} \simeq 500$ K and the other phase is the high-temperature orthorhombic (HO) one above T_{mo} [14]. In both cases the structures are completely different from that of

0953-8984/98/317003+11$19.50

the LM phase and are of a pseudobrookite-type built up by the linkage of distorted TiO_6 octahedra. The HO-phase Ti_3O_5 has been considered to be a highly correlated metal, where the effective Ti valence is nearly equal to the average value $\frac{10}{3}$ expected from the chemical formula, though it is difficult to obtain reliable transport properties owing to cracking of the specimens due to the large changes of the lattice constants at $T_{c1,2}$ as shown in table 1. The HO–HM transition is accompanied by a small magnetic anomaly, which may be attributed to Ti–Ti pair formation with a small gap and/or the distortion of octahedral units of oxygens in the framework of pseudobrookite-type structure. Here, the latter is inferred from the fact that the temperature-independent susceptibility of the LM-phase Ti_3O_5 is considerably smaller than that of the HO phase [14].

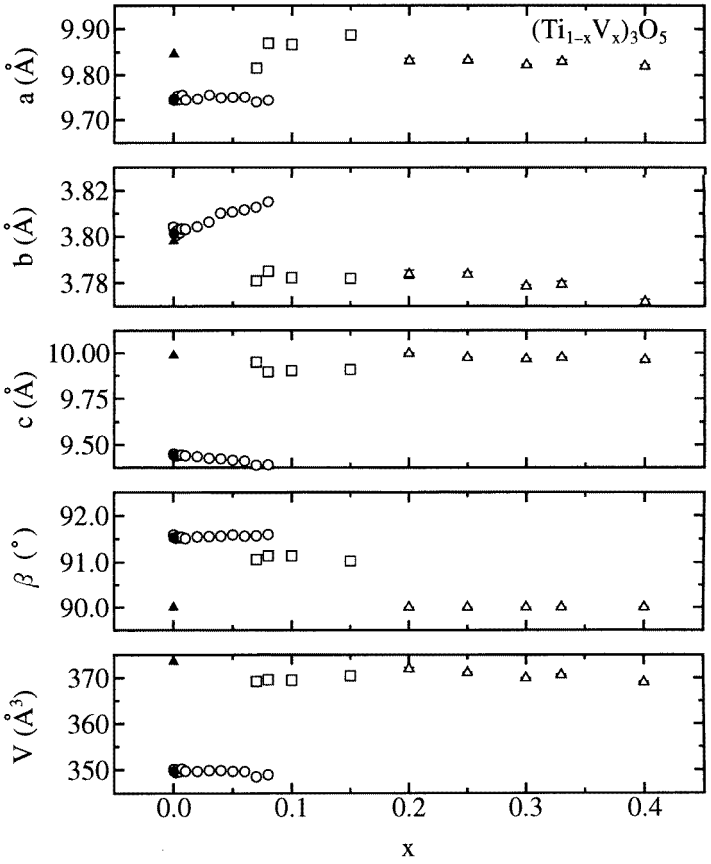

Figure 1. The x-dependence of the lattice constants for $(Ti_{1-x}V_x)_3O_5$ at 290 K, where the open circles, open squares, and open triangles indicate the low-temperature monoclinic phase, the high-temperature monoclinic one, and the high-temperature orthorhombic one, respectively. The full circles and full triangles at $x = 0$ show the data at 296 and 514 K, respectively, obtained from the x-ray four-circle diffraction [14].

The phase transition of Ti_3O_5 at $T_{c1,2}$ was found to be suppressed by a slight substitution of Fe for Ti [2]. The effects of doping with Sc, V, and Zr have also been investigated; the limits of solubility of these ions in the LM phase are 0.02, 0.07, and 0.08, respectively [12]. The main factor determining the reduction of $T_{c1,2}$ was attributed as the reduction of inequivalence in different crystallographic Ti positions. Previous investigations of the

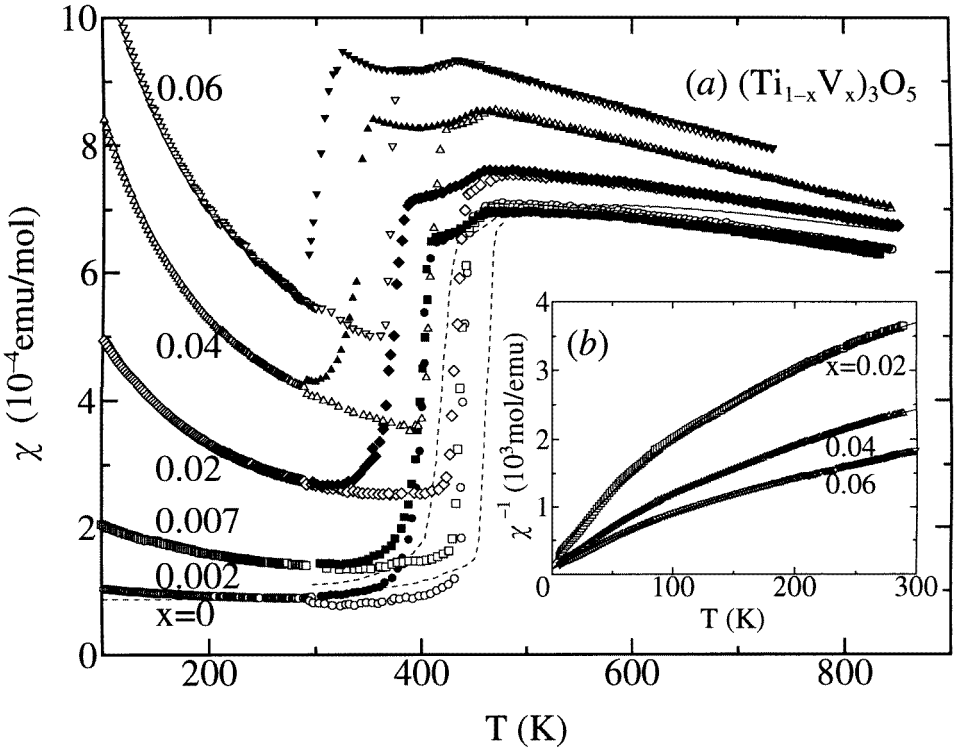

Figure 2. The temperature dependence of the magnetic susceptibility χ for $(Ti_{1-x}V_x)_3O_5$ with $0 \leqslant x \leqslant 0.06$: (*a*) χ against T between 100 and 850 K, where the open and full symbols are the data obtained on heating and cooling, respectively, and the dashed curves express data for $x = 0$ [14]; (*b*) χ^{-1} against T below 300 K, where the full curves indicate the results calculated on the basis of a Curie–Weiss law.

doping effect have concentrated on just electronic states for the low-temperature phase for compounds with transition to the LM phase. For compounds without structural transition, there are no data available.

It is important to further describe the electronic states of Ti_3O_5 with a pseudobrookite-type structure in the region above $T_{c1,2}$, since both an electron correlation and an electron–phonon coupling are expected to provide important contributions there. For this purpose, the $(Ti_{1-x}V_x)_3O_5$ system, where the composition $x = \frac{1}{3}$ has three electrons per formula unit with three cations, has been investigated on the basis of structural, magnetic, and transport properties. This may also allow us to explore in detail the main factor in the disappearance of $T_{c1,2}$. The experimental methods and the results are presented in sections 2 and 3, respectively. The electronic states for the high- and low-temperature phases are discussed in section 4, and section 5 is devoted to conclusions.

2. Experiments

Polycrystalline specimens of the $(Ti_{1-x}V_x)_3O_5$ system, where $0 \leqslant x \leqslant 0.4$, were prepared using an appropriate mixture of Ti (99.9% purity), TiO_2 (99.9% purity), and V_2O_5 (99.99% purity) with an Ar arc furnace. Electron-probe microanalysis (EPMA) was performed to

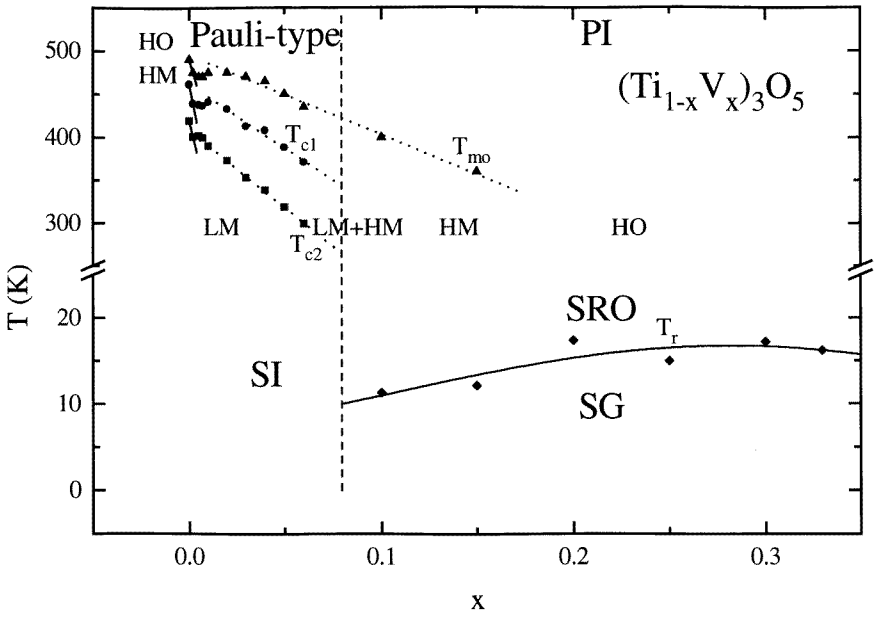

Figure 3. The phase diagram for $(Ti_{1-x}V_x)_3O_5$. Here, LM, HM, and HO show the low-temperature monoclinic phase, the high-temperature monoclinic one, and the high-temperature orthorhombic one, respectively. T_{c1} on heating and T_{c2} on cooling correspond to the HM–LM and spin-singlet transition temperatures, and T_{mo} indicates the HO–HM transition temperature. SI, PI, SRO, and SG show the phases of the spin-singlet insulator, the polaronic insulator, the short-range-ordered cluster, and the spin-glass, respectively. The lines and curves are drawn as guides to the eye.

estimate the cation concentration ratio.

X-ray powder diffraction patterns were obtained with Cu Kα radiation at 290 K by a two-circle diffractometer. The magnetization was obtained by the Faraday method with an applied field of up to 1 T in the temperature region between 4.2 and 1000 K, and the magnetic susceptibility was determined from the linear coefficient of magnetization versus field (M–H) curve with a decreasing field. The four-terminal electrical resistivity in the region between 100 and 600 K and the thermoelectric power in the region between 100 and 350 K were measured by a DC method.

3. Results

3.1. Lattice constants and the cation ratio

The cation concentration ratio V/Ti determined by EPMA agrees well with the nominal value.

At 290 K, the LM, HM, and HO phases are formed in the ranges of $0 \leqslant x \leqslant 0.06$, $0.1 \leqslant x \leqslant 0.15$, and $0.2 \leqslant x \leqslant 0.4$, respectively. The results for $x = 0.07$ and 0.08 indicate a mixture of the LM and HM phases. The x-range for the LM phase is fairly consistent with the previous result [12]. The lattice constants of the LM, HM, and HO phases against x are shown in figure 1 by the open circles, open squares, and open triangles, respectively. For comparison, the results for the LM and HO phases for $x = 0$ determined by means of

the single-crystal diffraction are indicated by the full circles and full triangles, respectively. Here, it should be noted that the lattice constants a, b, and β in the LM and HM phases correspond to b, a, and α in the HO phase, respectively. The behaviours as a function of x are very similar to those against temperature for the composition Ti_3O_5 [14], i.e. the addition of V is approximately equivalent to the increase of temperature. The compounds with $x = 0.07$ and 0.08 undergo first-order phase transitions at around room temperature.

3.2. Magnetic properties

3.2.1. Susceptibility for $0 \leqslant x \leqslant 0.06$. The temperature dependence of the magnetic susceptibility χ for $0 \leqslant x \leqslant 0.06$ between 100 and 850 K, and that of χ^{-1} below 300 K are shown in figures 2(a) and 2(b), respectively. Here, the open and full symbols in figure 2(a) indicate the data obtained on heating and cooling, respectively, and the dashed curves show previously obtained data for the composition Ti_3O_5 [14]. All of the data for this x-range exhibit first-order magnetic transitions at $T_{c1,2}$. As shown in figure 3, the reduction of $T_{c1,2}$ for $x = 0.002$ is very significant, but for $0.002 < x \leqslant 0.01$, it is nearly constant. For $x > 0.01$, $T_{c1,2}$ decreases monotonically with x. There is another *reversible* transition temperature at which χ has a cusp above $T_{c1,2}$. On the basis of the result for Ti_3O_5 [14], this temperature is considered to correspond to T_{mo} for the high-temperature phase. As indicated in figure 3, T_{mo} has an x-dependence similar to that of $T_{c1,2}$, but it reaches up to $x = 0.15$. Thus, for $x \leqslant 0.06$, three characteristic temperature regions are defined: $T < T_{c1,2}$, $T_{c1,2} < T < T_{mo}$, and $T_{mo} < T$.

Below $T_{c1,2}$, χ shows a Curie–Weiss paramagnetism without magnetic order in the region for which measurements were made: $\chi = C/(T + T_W) + \chi_0$, where C, T_W, and χ_0 are the Curie constant, the Weiss temperature, and the temperature-independent contribution of the Van Vleck orbital and diamagnetic susceptibilities, respectively. The full curves in figure 2(b) show the results calculated on the basis of the parameters plotted in figure 4. Here, C increases monotonically with x. For $x \leqslant 0.01$, T_W is close to zero and χ_0 is nearly constant, while for $x > 0.01$, they increase with x.

At temperatures between $T_{c1,2}$ and T_{mo}, χ for $x \leqslant 0.03$ decreases gradually with decreasing temperature. On the other hand, χ for the larger x shows a slight upturn at intermediate temperatures. In the region above T_{mo}, χ with $x = 0$ is of the Pauli type with the Fermi energy $E_F \simeq 2 \times 10^3$ K and the effective electron mass $m^* \simeq 16m_0$, m_0 being a free-electron mass [14]. The thermal variation of χ for $x \neq 0$ is apparently larger than that for $x = 0$. The x-dependence of χ at the fixed temperatures above T_{mo} has a minimum at $x \simeq 0.01$.

3.2.2. Susceptibility and remanent magnetization for $0.1 \leqslant x \leqslant 0.33$. The temperature dependence of the inverse magnetic susceptibility χ^{-1} for $0.1 \leqslant x \leqslant 0.33$ between 4.2 and 1000 K is shown in figure 5(a). It apparently shows a ferrimagnetic-like behaviour. For $x = 0.1$ and 0.15, small magnetic anomalies take place at about 400 and 360 K, respectively, which may be attributed to the HO–HM transitions as shown in figure 3 by the full triangles. χ above T_{mo} for $x = 0.10$ and 0.15 and that above 100 K for $0.15 < x \leqslant 0.33$ follow the Curie–Weiss law. The full curves in figure 5(a) show the values calculated with the parameters plotted in figure 4. Both C and χ_0 are roughly proportional to x. T_W decreases rapidly with increasing x in the range $0.1 \leqslant x \leqslant 0.2$, but for larger x, it is nearly constant.

χ below T_{mo} for $x = 0.10$ and 0.15 and that below about 100 K for $0.15 < x \leqslant 0.33$ deviate significantly from the Curie–Weiss curves obtained above. With the transition temperature T_r at around which χ has a peak as plotted in figure 3 as the full diamond, the

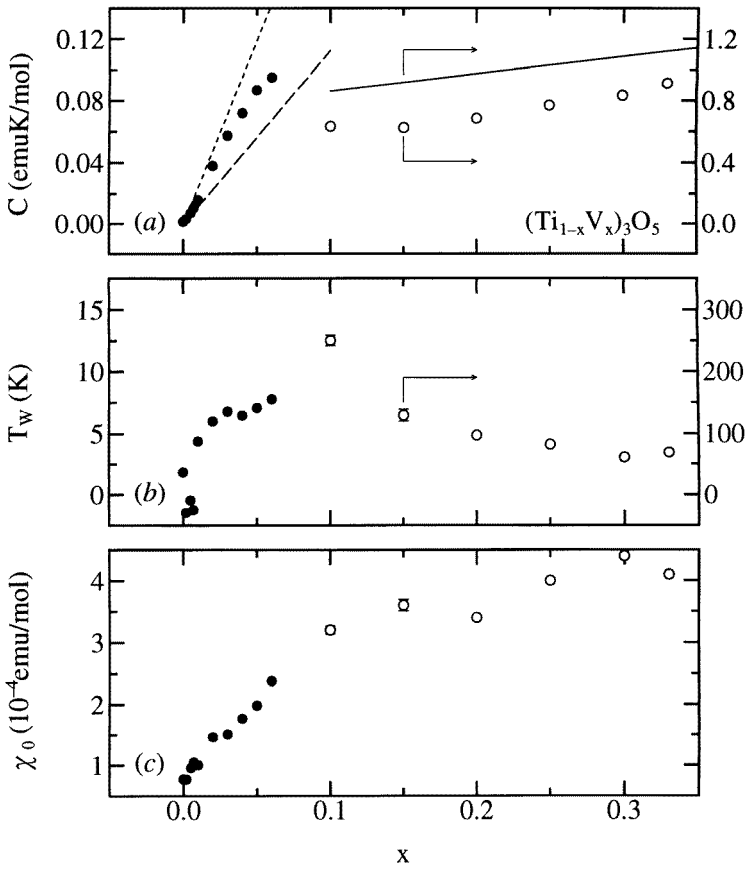

Figure 4. The x-dependences of (a) the Curie constant C, (b) the Weiss temperature T_W, and (c) the temperature-independent susceptibility χ_0 for $(Ti_{1-x}V_x)_3O_5$. Here, the full and open circles show the results for the LM phase ($0 < x \leqslant 0.06$) and for the HO phase ($0.1 \leqslant x \leqslant 0.33$), respectively. The lines in (a) indicate the calculated results.

remanent magnetization σ defined by $M = \chi H + \sigma$ appears. The temperature dependence of σ is shown in figure 5(b). This behaviour is weaker than that expected from the weak ferromagnetism, $\sigma/\sigma_0 = \tanh[\sigma T_r/(\sigma_0 T)]$, where σ_0 is the value at 0 K. The magnitude of σ is rather small and does not depend significantly on x.

3.3. Transport properties

The electrical conductivity below $T_{c1,2}$ for the single crystals of Ti_3O_5 is like that in a semiconductor or a variable-range hopping, but at around $T_{c1,2}$, it increases more than tenfold [14]. Below $T_{c1,2}$, the temperature dependence of the resistivity for the polycrystalline compounds with $0 < x \leqslant 0.06$ is roughly similar to that of the composition Ti_3O_5 with an activation energy of about 2×10^3 K. Unfortunately, it is difficult to obtain precise results for the electrical resistivity above $T_{c1,2}$ owing to cracking of the specimens at the transition. However, at least it can be said that the resistivity for this x-range decreases rapidly at around $T_{c1,2}$ on heating.

The electrical resistivity ρ for $0.1 \leqslant x \leqslant 0.33$ as a function of T^{-1} is shown in

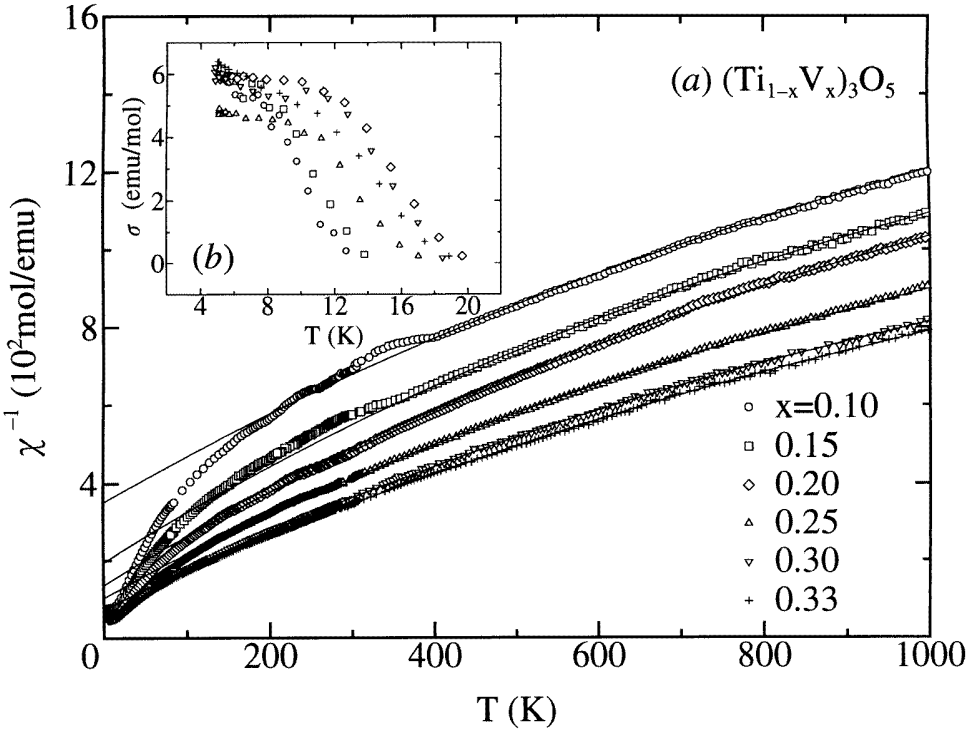

Figure 5. The temperature dependences of (*a*) the inverse magnetic susceptibility χ^{-1} and (*b*) the remanent magnetization σ for $(Ti_{1-x}V_x)_3O_5$ with $0.1 \leqslant x \leqslant 0.33$. The full curves in (*a*) indicate the results calculated on the basis of a Curie–Weiss law.

figure 6(*a*). In this x-range, no electrical anomalies due to the HM–LM transition are obtained, which is consistent with the results on magnetic properties. The temperature dependence is like that of a semiconductor. The activation energy E_g/k defined as $\rho = \rho_0 \exp(E_g/kT)$, where ρ_0 is assumed to be a constant and k is the Boltzmann constant, is of the order of 2×10^3 K from the full lines in figure 6(*a*), which is comparable with the value for the LM phase. The curves representing the resistivity data for $x = 0.10$ and 0.15 at low temperatures bend downwards with decreasing temperature; this may be caused by a three-dimensional variable-range-hopping conduction, $\ln \rho \propto T^{-1/4}$ [15].

The thermoelectric power S for $0.1 \leqslant x \leqslant 0.33$ against T^{-1} is shown in figure 6(*b*). Above 250 K, S seems to have a term proportional to T^{-1}. On the other hand, below 200 K, it is nearly constant and the absolute value decreases with increasing x. The negative sign of S suggests an electron carrier and S below 200 K for $x = 0.33$ is approximately zero. This result is clearly different from the behaviour expected from a wide-band semiconductor model.

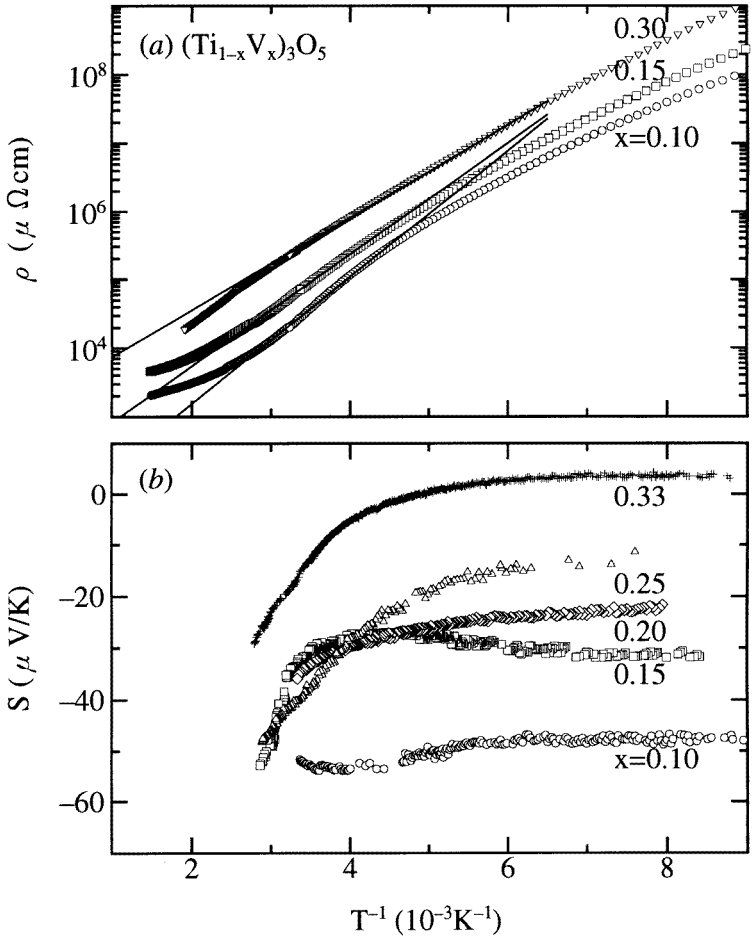

Figure 6. The temperature dependences of (*a*) the electrical resistivity ρ and (*b*) the thermoelectric power S for $(Ti_{1-x}V_x)_3O_5$ with $0.1 \leqslant x \leqslant 0.33$. The full lines in (*a*) indicate the results calculated on the basis of a semiconductor model.

4. Discussion

4.1. Electronic states with $0 \leqslant x \leqslant 0.08$

The results on the structural, magnetic, and transport properties show that the compounds with $0 \leqslant x \leqslant 0.08$ undergo a transition to the LM phase at $T_{c1,2}$. The exchange constant for paramagnetic ions in the LM phase is rather small, so they may be isolated. The significant reduction of $T_{c1,2}$ for $x = 0.002$ suggests that V ions in this small x-range are partly in the trivalent state, since we know that the reduction due to the doping with trivalent ions, irrespective of whether they are magnetic or nonmagnetic, is larger than that with tetravalent ions [2, 12]. One can also expect the isolated V ions for $0.01 < x \leqslant 0.08$ in the LM phase to be mostly in the tetravalent state, since the x-dependence of $T_{c1,2}$ for this x-range is similar to the result of the nonmagnetic Zr^{4+} doping [12]. Thus, the behaviour of $T_{c1,2}$ for $0.002 < x \leqslant 0.01$ may be attributed to the change in the V valence as previously suggested on the basis of differential-thermal-analysis data [12]. The x-dependences of the Curie

constants for the doped V ions with the ratio $V^{3+}/V^{4+} = 2$ (the same case as in Ti_3O_5) and with only V^{4+} ions are indicated in figure 4(*a*) by the dotted and broken lines, respectively, where $g = 2$. The above model may prove to be correct. Unfortunately, further discussion on this point is difficult, since a possible contribution from the isolated paramagnetic Ti ions induced by the doping should also be considered.

χ_0 in the LM phase corresponds to the temperature-independent susceptibility originating from the spin-singlet pairs and the isolated ions. As mentioned earlier, χ_0 in the LM phase of Ti_3O_5 is considerably smaller than that in the HO phase [14]. Thus, the fact that, for $x > 0.01$, χ_0 increases with x and tends towards the value extrapolated from the composition without transition to the LM phase suggests that the crystal-field effect in the octahedral unit of oxygens in the LM phase becomes similar to that in the HO phase with increase of x. This probably makes the valence order state there incomplete. Another explanation is that a proportion of the magnetic ions that do not form the spin-singlet pairs have a nearly temperature-independent spin susceptibility, but this is unlikely.

The difference of χ with $x \neq 0$ from that with $x = 0$ above T_{mo} is negative for $0 < x \leqslant 0.01$ and positive for $x > 0.01$ as described earlier. This is probably caused by a difference between the valences of the V ions. The exchange interaction for V ions in the HO and HM phases may be still small, neglecting possible indirect couplings due to the RKKY interaction [16]. The temperature-dependent contribution in the LM phase should be superposed on the susceptibility χ^* in the HO and HM phases which exhibits the magnetic transition. In other words, the Ti ions that form local spin-singlet pairs below $T_{c1,2}$ and the isolated paramagnetic ions may coexist in the HO and HM phases. Using the parameters shown in figure 4, one finds that the temperature dependence of χ^* is of the Pauli type rather than of the Curie–Weiss type. On the assumption that χ_0 in the HO phase is given by the value extrapolated from the larger-x side, χ^* is found to be reduced with x for $0 \leqslant x \leqslant 0.01$, outside of which range the reduction is not significant. This result may be consistent with the above model; i.e. for $x > 0.01$, the V^{4+}–Ti^{4+} substitution is dominant, and, therefore, the number of Ti^{3+} ions that form the spin-singlet pairs does not change significantly. It is not clear whether or not the HO-phase compounds with $x \neq 0$ are metallic, since the disorder effect due to the doping may cause an electron localization, and the correlation effect comparable with the bandwidth often leads to variable-range-hopping transport states [17].

4.2. Electronic states with $0.1 \leqslant x \leqslant 0.33$

The electrical resistivity for $0.1 \leqslant x \leqslant 0.33$ has an activation-type thermal variation, while the thermoelectric power at low temperatures is small and depends little on temperature. Assuming that the estimated activation energy corresponds to the energy for electron hopping in the localized states, carriers in this x-range are suggested to enter self-trapped or polaronic states.

On the basis of the x-dependence of the Curie constant for $0.1 \leqslant x \leqslant 0.33$ shown in figure 4(*a*), it is suggested that all of the paramagnetic ions are localized and the V ions are in the state V^{4+} with $3d^1$ as indicated by the full line, where $C = 0.75 + 1.12x$ with $g = 2$. Moreover, the result that the Weiss temperature is much larger than that for $0 \leqslant x \leqslant 0.08$ indicates that the exchange interaction between Ti^{3+} and V^{4+} ions is significant because of the relatively high concentration of V ions as well as the strong localization due to the disorder [18]. Thus, the magnetic properties are completely different from those of the HO phase for $0 \leqslant x \leqslant 0.08$. From the result for χ_0 shown in figure 4(*c*), the crystal-field effect for the octahedral unit of oxygens does not change significantly. Here, it is noted that

the extrapolated value at $x = 0$, $\chi_0 \simeq 2.8 \times 10^{-4}$ emu mol^{-1}, agrees well with the value obtained from the free-electron-model analysis [14].

A significant difference between the measured susceptibility and the Curie–Weiss curve calculated from the high-temperature side is not ascribed to the magnetic impurity or lattice imperfection by considering the x-ray diffraction result. It may be attributed to the formation of short-range-ordered clusters with the antiferromagnetic correlation due to the disorder and the competition of different superexchange interactions as expected from the crystal structure. The occurrence of the remanent magnetization is probably due to the freezing of the clusters, since the composition dependence of T_r is rather small: i.e. T_r may correspond to the transition temperature to the spin-glass-like phase. It should be noted that the related compound Fe_2TiO_5 exhibits anisotropic spin-glass behaviour [19]. The HO–HM transition occurs even when the susceptibility is of the Curie–Weiss type, where the Weiss temperature is apparently large.

5. Conclusion

The effect of V doping on the electronic states and the phase transitions of Ti_3O_5 has been investigated on the basis of structural, magnetic, and transport properties. Analysis of our data leads to the phase diagram shown in figure 3 with several critical parameters and properties. There exist three structural phases as functions of x and temperature: the high-temperature orthorhombic (HO) phase with a pseudobrookite-type structure and the slightly deformed monoclinic (HM) one, and the low-temperature monoclinic (LM) one.

For $0 \leqslant x \leqslant 0.08$, the HO–HM and HM–LM transitions successively take place at T_{mo} and at T_{c1} (T_{c2}) on heating (cooling), respectively. The magnetic properties for this x-range are considered as contributions from the Ti ions that form the spin-singlet pairs in the LM insulator phase (SI) and the isolated ions due to the doping. At $x \simeq 0.01$, the valence of doped V ions may change. For $0.01 < x \leqslant 0.08$, the doping can transform the octahedral unit of oxygens in the LM phase into a unit similar to that of the HO phase without significant change of the mass-enhanced susceptibility. This probably weakens the effect of valence order in the LM phase, which leads to the reduction of $T_{c1,2}$. The HO-phase Ti_3O_5 is like a highly correlated metal, but it is not clear whether the HO-phase compounds with $0 < x \leqslant 0.08$ with apparent Pauli-type susceptibility and the delocalized density of states have a metallic state or a variable-range-hopping one.

The HO-phase compounds with $0.1 \leqslant x \leqslant 0.33$ are interpreted as being strongly localized and polaronic insulators (PI), where only Ti^{4+} ions are substituted for with V^{4+}, and a mixed-oxide model in which the Ti ions and the doped ones interact with each other may be applied. Thus, the abrupt disappearance of $T_{c1,2}$ may be caused by a localization effect of electrons due to the disorder as well as an electron–phonon coupling effect. This idea supports experimental evidence that the composition dependence of $T_{c1,2}$ for the V^{4+} doping is similar to that for the Zr^{4+} doping except for a very small x-range. The PI phase exhibits short-range-ordered (SRO) spin-correlation effects and the spin-glass-like (SG) phase appears at low temperatures below T_r. The presence of the SG phase above $x \simeq 0.1$ is correlated with the disappearance of $T_{c1,2}$, since in the LM phase, only the exchange coupling within the Ti–Ti pair is significant. In order to explain quantitatively a crossover from the delocalized state to the strongly localized one at around $x \simeq 0.1$, further work is necessary.

Acknowledgment

We thank Professor D S Hirashima for useful discussions.

References

[1] See, for example,
Mott N F 1990 *Metal–Insulator Transitions* 2nd edn (London: Taylor & Francis)
[2] Åsbrink S and Magnéli A 1959 *Acta Crystallogr.* **12** 575
[3] Ždanov G S and Rusakov A A 1954 *Struct. Rep.* **18** 459
Ždanov G S and Rusakov A A 1954 *Trudy Inst. Kristallogr. Akad. Nauk SSSR* **9** 165
[4] Andersson S, Collén B, Kruuse G, Kuylenstierna U, Magnéli A, Pestmalis H and Åsbrink S 1957 *Acta Chem. Scand.* **11** 1653
[5] Åsbrink G and Magnéli A 1967 *Acta Chem. Scand.* **21** 1977
[6] Bartholomew K F and Frankl D R 1969 *Phys. Rev.* **187** 828
[7] Iwasaki H, Bright N F H and Rowland J F 1969 *J. Less-Common Met.* **17** 99
[8] Mulay L N and Danley W J 1970 *J. Appl. Phys.* **41** 877
[9] Rao C N R, Ramdas S, Loehman R E and Honig J M 1971 *J. Solid State Chem.* **3** 83
[10] Åsbrink S and Pietraszko A 1991 *Phys. Status Solidi* a **128** K77
[11] Kellerman D G, Perelyaev V A and Shveikin G P 1983 *Inorg. Mater.* **19** 218
[12] Kellerman D G, Zhilyaev V A, Perelyaev V A and Shveikin G P 1983 *Inorg. Mater.* **19** 221
[13] Kellerman D G, Zainulin Y G and Perelyaev V A 1983 *Inorg. Mater.* **19** 305
[14] Onoda M 1998 *J. Solid State Chem.* **136** 67
[15] Brenig W, Döhler G H and Wölfle P 1973 *Z. Phys.* **258** 381
[16] See, for example,
Moriya T 1985 *Spin Fluctuations in Itinerant Electron Magnetism* (Berlin: Springer) ch 8
[17] Onoda M and Kohno M 1998 *J. Phys.: Condens. Matter* **10** 1003 and references therein
[18] See, for example,
Siringo F 1995 *Condensed Matter—Disordered Solids* ed S K Srivastava and N H March (London: World Scientific) ch 7
[19] Atzmony U, Gurewitz E, Melamud M, Pinto H, Shaked H, Gorodetsky G, Hermon E, Hornreich R M, Shtrikman S and Wanklyn B 1979 *Phys. Rev. Lett.* **43** 782